\



Synthesis and study the influence of yttrium doping on band structure, optical, non-linear optical and dielectric results for $Ca_{12}Al_{14}O_{33}$ (C12A7) single crystals grown using traveling-solvent floating zone (TSFZ) method

A. Abdel Moez, A.hmed I. Ali, and A. Tayel

Citation: Chin. Phys. B, 2022, 31 (**1**): 018103. DOI: 10.1088/1674-1056/ac0a5f
Journal homepage: http://cpb.iphy.ac.cn; http://iopscience.iop.org/cpb

What follows is a list of articles you may be interested in

Overview of finite elements simulation of temperature profile to estimate properties of materials 3D-printed by laser powder-bed fusion

Habimana Jean Willy, Xinwei Li(李辛未), Yong Hao Tan, Zhe Chen(陈哲), Mehmet Cagirici, Ramadan Borayek, Tun Seng Herng, Chun Yee Aaron Ong, Chaojiang Li(李朝将), Jun Ding(丁军)
Chin. Phys. B, 2020, 29 (**4**): 048101. DOI: 10.1088/1674-1056/ab6d4e

Dislocation distributions and tilts in Al(Ga)InAs reverse-graded layers grown on misorientated GaAs substrates

Yang He(何洋), Yu-run Sun(孙玉润), Yongming Zhao(赵勇明), Shuzhen Yu(于淑珍), Jianrong Dong(董建荣)
Chin. Phys. B, 2017, 26 (**3**): 038102. DOI: 10.1088/1674-1056/26/3/038102

Control of symmetric properties of metamorphic $In_{0.27}Ga_{0.73}As$ layers by substrate misorientation

Shu-Zhen Yu(于淑珍), Jian-Rong Dong(董建荣), Yu-Run Sun(孙玉润), Kui-Long Li(李奎龙),Xu-Lu Zeng(曾徐路), Yong-Ming Zhao(赵勇明), Hui Yang(杨辉)
Chin. Phys. B, 2016, 25 (**3**): 038101. DOI: 10.1088/1674-1056/25/3/038101

A superhigh discharge capacity induced by a synergetic effect between high-surface-area carbons and a carbon paper current collector in a lithium–oxygen battery

Luo Guang-Sheng, Huang Shi-Ting, Zhao Ning, Cui Zhong-Hui, Guo Xiang-Xin
Chin. Phys. B, 2015, 24 (**8**): 088102. DOI: 10.1088/1674-1056/24/8/088102

Fabrication and characterization of direct-written 3D TiO_2 woodpile electromagnetic bandgap structures

Li Ji-Jiao, Li Bo, Peng Qin-Mei, Zhou Ji, Li Long-Tu
Chin. Phys. B, 2014, 23 (**9**): 098104. DOI: 10.1088/1674-1056/23/9/098104

Synthesis and study the influence of yttrium doping on band structure, optical, non-linear optical and dielectric results for $Ca_{12}Al_{14}O_{33}$ (C12A7) single crystals grown using traveling-solvent floating zone (TSFZ) method

A. Abdel Moez[1,†], Ahmed I. Ali[2], and A. Tayel[2]

[1] *Solid State Physics Department, Physical Research Division, National Research Centre (NRC), 33 El Bohouth Street, Dokki, Giza* 12622, *Egypt*
[2] *Basic Science Department, Faculty of Faculty of Technology and Education, Helwan University, Kobry El-Qopa, Cairo* 11281, *Egypt*

(Received 15 April 2021; revised manuscript received 17 May 2021; accepted manuscript online 11 June 2021)

$Ca_{12}Al_{14}O_{33}$ (C12A7) and $Y_{0.02}Ca_{11.98}Al_{14}O_{33}$ (Y-C12A7) single crystals were grown by using the traveling-solvent floating zone (TSFZ) method. The temperature was increased to avoid the bubbles and cracks which may be formed during the preparation of the ingot material. We have started with the flux higher than the normal to avoid the bubbles and make good treatment for the solid-liquid interface. The structures of both $Ca_{12}Al_{14}O_{33}$ (C12A7) and $Y_{0.02}Ca_{11.98}Al_{14}O_{33}$ (Y-C12A7) were studied by using x-ray diffraction (XRD). Optical properties for C12A7 and Y-C12A7 single crystals have been studied in order to determine the optical parameters such as optical energy gap (E_g), refractive index n, oscillating energy (E_o), dispersion energy (E_d), volume energy loss function (VELF), and surface energy loss function (SELF). Finally, a new result for these samples is that the third-order nonlinear optical susceptibility ($\chi^{(3)}$) was determined. The results have been discussed with effect of Y-doping on the C12A7 single crystals for optical and industrial applications.

Keywords: syntheses $Ca_{12}Al_{14}O_{33}$ (C12A7) single crystals, Y-doping, optical parameters, dielectric results, nonlinear optical susceptibility

PACS: 81.05.–t

DOI: 10.1088/1674-1056/ac0a5f

1. Introduction

Because of their importance in electronics applications and their common use in modern technology,[1,2] calcium aluminates have been widely and successfully used for the construction[3] of luminescent materials.[4–6] Calcium aluminates glasses have attracted attention of the scientists because of their unique properties,[7] such as optical and mechanical properties.[8,9] Due to their properties, these materials are widely used in many electronics and bone applications.[10,11] There are many methods for preparing $Ca_{12}Al_{14}O_{33}$ crystals (C12A7) including the solvent floating zone method (SFZM)[12] that gives high quality single crystals, self-propagating combustion method, solid state reaction,[13] citric acid and the sol–gel combustion method.[14] More $CaA_{l4}O_7$ single crystals were synthesized by the citric acid precursor method.[15] The crystal structure of $Ca_{12}Al_{14}O_{33}$ (C12A7) is cubic ($a_o = 11.982$ Å,[16] and C12A7 is known as an oxygen ionic conductor).[17] Many authors found that C12A7 has only one crystal structure, which has four positive charges with O_2 anions.[18–20] C12A7 crystals have body-centered cubic structure.[21,22] Moreover, the defect structure of C12A7 was studied[23–25] to describe the chemical defects.

The physical properties of C12A7 have been studied widely such as the electric properties,[26] thermodynamic[27] and optical properties.[28] The influence of doping of Er-ion on both of structure and Raman absorption spectra for 12Ca7Al powders have been studied,[29] and it was noticed that, the optical properties depend on the phase transformation of the Ca–Al–O system.[30] The effect of Eu-dopant on the blue emission of $12CaO{\cdot}7Al_2O_3$ thin films was reported[31] that Eu films exhibit blue emission peak at 444 nm, while it was found that $CaAl_2O_4$ doped with Er^{3+} exhibits emission band at 523 nm and 547 nm,[32] and also Eu^{2+} ion affects on the absorption spectra for $Ca_{12}Al_{10}{\cdot}6Si_3{\cdot}4O_{32}Cl_{5.4}$.[33] Moreover, Eu effects the optical emission spectra for $CaAl_2O_4$ samples.[34] The effect of temperature on the physical properties of $CaAl_4O_7$ doped with Eu^{3+} was studied[35,36] and found the sample with photoluminescence spectrum from 340 nm to 420 nm[35] also had emitted green and red up-conversion emissions.[36] While the effect of doping with Nd^{3+}/Yb^{3+} in co-doped $Ca_{12}Al_{14}O_3$ on both of down conversion (DC) and up conversion (UC) processes have been investigated,[37] and the influence of doped with Mn^{+4} ion on the luminescent properties of $CaAl_4O_7$ powder[38,39] and fluorescence properties[40] was studied.

In this paper, single crystals of $Ca_{12}Al_{14}O_{33}$ (C12A7) and $Y_{0.02}Ca_{11.98}Al_{14}O_{33}$ (Y-C12A7) have been generated by using the traveling-solvent floating zone method (TSFZ). XRD is used to characterize the single crystals. Optical measurements such as transmission (T) and reflection (R) have been carried out for C12A7 and Y-doped C12A7 single crystals to calculate the optical parameters such as optical energy gap, n, E_o, E_d, VELF, and SELF. Moreover, the third-order nonlinear

†Corresponding author. E-mail: aam692003@yahoo.com

© 2022 Chinese Physical Society and IOP Publishing Ltd

optical susceptibility ($\chi^{(3)}$) has been estimated.

2. Experimental work

2.1. Ingot material preparation

C12A7 polycrystalline samples were carefully fabricated to avoid extrinsic (impurity) effects by using high-purity chemicals $CaCO_3$ (99.995% Aldrich) and Al_2O_3 (99.99% Aldrich). Powders of $CaCO_3$, Al_2O_3 and Y_2O_3 were mixed for preparations of stoichiometric $Ca_{12}Al_{14}O_{33}$ (C12A7) and $Y_{0.02}Ca_{11.98}Al_{14}O_{33}$ (Y-C12A7) polycrystalline. The mixed powder was ground well and heated up to 1100 °C with oxygen flow for 24 hours. The powders was ground again and put into a rubber tubes, then pressed under a hydrostatic pressure of 300 MPa to form a rod shape. The pressed rods were sintered at 1250 °C in oxygen flow for 12 hours.

2.2. The traveling floating zone melting technique

The sintered polycrystalline rods were used as feed and seed for single crystals. The conditions of the typical growth run were as follows: The growth rate was 0.3 mm/h–0.4 mm/h, and the polycrystalline rod and growing crystal rod were rotated at 25 rpm and 20 rpm in direction opposite to each other, respectively. It was also found that the bubbles and cracks were decreased with high temperature for the crystal. The surfaces for these single crystals were investigated to avoid the effects of grain boundaries and surfaces. The polycrystalline and single-crystal samples were heated at 1300 °C for 2 h in presence of mixing gas of 20% H_2/80% N_2, and finally these crystals were rapidly cooled to room temperature. The crystal structure analysis was carried out by using x-ray diffraction of type (XRD; Rigaku, D/MAXRc) with Cu $K\alpha$ radiation at a wavelength of 1.54 Å. The optical measurements such as transmission and reflection spectra of the single crystals samples were measured by using UV/VIS double-beam spectrophotometer of type (Cary 5E).

3. Results and discussion

3.1. Structure

XRD results of C12A7 and Y-C12A7 single crystals are shown in Fig. 1. It was found that the doping affected on both the peaks intensity and a full width at half maximum (FWHM) of these studied samples.

The crystallite size C_s of these crystals has been calculated as[41]

$$C_s = \frac{0.9\lambda}{\beta \cos\theta}, \tag{1}$$

while the dislocation density ρ, which refers to the number of defects in the crystal, is determined by[42]

$$\rho = \frac{1}{C_s^2}. \tag{2}$$

The lattice strain L_s was calculated by using[43]

$$L_s = \frac{\beta \cos\theta}{4}. \tag{3}$$

The number of crystallites per unit area N of the studied crystals was determined as[44]

$$N = \frac{d}{C_s^3}, \tag{4}$$

where d is the crystal thickness. The calculated values for these crystals studied here are shown in Table 1.

Table 1. The structure determined values such as β, C_s, ρ, N and L_s.

Y-Ca12A7 single crystals					C12A7 single crystals					
L_s	N (cm^{-2})	ρ (line/cm^2)	C_s (nm)	β (FWHM)	L_s	N (cm^{-2})	ρ (line/cm^2)	C_s (nm)	β (FWHM)	Θ
0.90	6.70×10^{18}	2.00×10^{15}	045.00	00.06	02.40	3.20×10^{15}	5.20×10^{8}	044.00	0.060	11.56
0.02	1.80×10^{16}	3.00×10^{20}	170.00	00.03	02.80	3.20×10^{13}	3.10×10^{8}	120.00	0.030	14.14
0.64	3.70×10^{18}	6.70×10^{15}	081.00	00.03	00.68	5.70×10^{14}	2.40×10^{8}	072.00	0.028	18.08
1.31	4.40×10^{18}	4.70×10^{15}	068.00	00.02	00.25	9.30×10^{14}	2.50×10^{8}	069.00	0.023	21.58
0.33	2.00×10^{18}	2.40×10^{16}	154.00	00.01	00.48	8.10×10^{13}	9.30×10^{7}	100.00	0.020	25.9
0.10	8.00×10^{17}	1.43×10^{17}	378.00	00.02	03.40	5.50×10^{12}	8.20×10^{7}	346.00	0.024	30.02
0.04	3.30×10^{17}	8.20×10^{17}	906.00	00.03	14.10	4.00×10^{11}	1.10×10^{8}	906.00	0.030	33.04
0.16	1.20×10^{18}	6.50×10^{16}	254.00	00.01	00.71	1.80×10^{13}	1.80×10^{7}	236.00	0.014	33.44
0.16	1.20×10^{18}	6.10×10^{16}	246.00	00.01	00.79	2.00×10^{13}	2.90×10^{7}	200.00	0.016	35.66
0.24	1.70×10^{18}	3.20×10^{16}	178.00	00.02	00.58	5.30×10^{13}	3.80×10^{7}	178.00	0.015	41.84
0.66	2.60×10^{18}	1.40×10^{16}	117.00	00.01	00.20	1.90×10^{14}	8.10×10^{7}	109.00	0.015	47.61
0.55	3.10×10^{18}	9.10×10^{15}	095.00	00.02	00.50	3.40×10^{14}	1.10×10^{8}	95.00	0.021	49.50
0.14	1.20×10^{18}	6.80×10^{16}	260.00	00.02	02.60	1.70×10^{13}	1.40×10^{7}	250.00	0.025	55.20
1.10	2.20×10^{18}	1.83×10^{16}	135.00	00.01	00.10	1.20×10^{14}	6.50×10^{7}	125.00	0.012	56.30
2.20	3.30×10^{18}	8.45×10^{15}	092.00	00.02	00.01	3.70×10^{14}	1.50×10^{8}	082.00	0.018	56.40
0.26	1.70×10^{18}	3.10×10^{16}	177.00	00.01	00.40	5.40×10^{13}	3.20×10^{7}	177.00	0.013	57.40
0.19	1.30×10^{18}	5.40×10^{20}	233.00	00.01	0.44	2.40×10^{13}	2.10×10^{7}	215.00	0.012	57.50
4.67	8.10×10^{18}	1.40×10^{15}	037.00	00.04	0.21	5.60×10^{15}	7.30×10^{8}	037.00	0.040	59.48

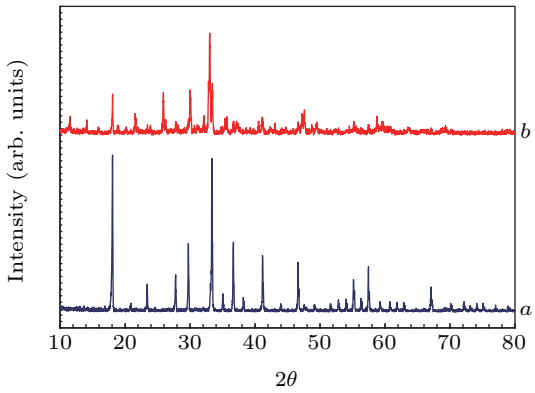


Fig. 1. XRD analysis for C12A7 (*a*) and Y-Ca12A7 (*b*) single crystals.

3.2. Optical results

Both of T and R spectra for these investigated samples are shown in Figs. 2(a) and 2(b). From Fig. 2(a) it was noticed that these samples had the same behavior for T, but Y-Ca12A7 sample has a higher values of T than $Ca_{12}Al_{14}O_{33}$ sample, and on the other hand the behavior of R for these crystals are completely different from each other as shown in Fig. 3(b). While Y-Ca12A7 had a lower value of R than Ca12A7, and this could be attributed that the yttrium (Y) is an element and has a dark-gray color, which increases the probability of absorption and decreases both of T and R.

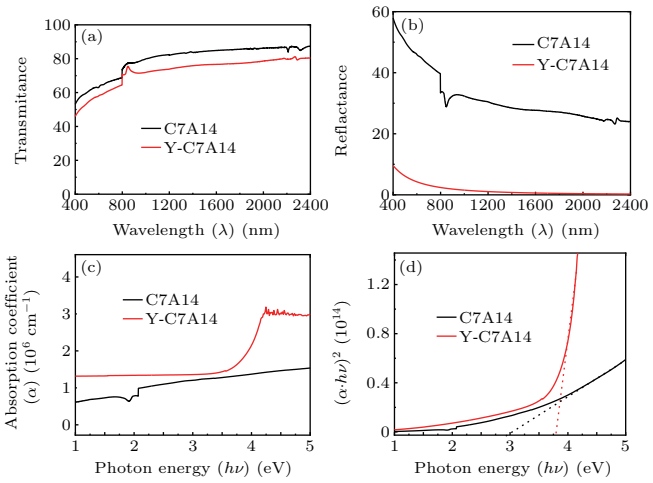


Fig. 2. The optical properties of C12A7 and Y-Ca12A7 single crystals: (a) the transmittance T, (b) the reflectance R, (c) the absorption coefficient α dependence on the photon energy and (d) the relation between $(\alpha \cdot h\nu)^2$ and photon energy $h\nu$.

The optical energy gap (E_g) is determined from the absorption curves as[45]

$$\alpha = A(h\nu - E_g)^p, \tag{5}$$

where A is a constant and α is the absorption coefficient determined as[46]

$$\alpha = \left(\frac{1}{d}\right) \ln\left(\frac{(1-R)^2}{T}\right). \tag{6}$$

The dependence of α on the photon energy $h\nu$ for these crystals studied is shown in Fig. 2(d). Direct energy gap E_{gdirc} was determined by the extrapolation of the linear part of the curves as shown in Fig. 2(d). It was found that the E_{gdirc} for C12A7 was 3.00 eV, while for Y-Ca12A7 was 3.80 eV, and this could be attributed to that the electron mobility for C12A7 is higher than the electron mobility of Y-Ca12A7 crystals, and these electrons mobility affect on the conductivity of these studied samples, which finally decrease the E_{gdirc}.

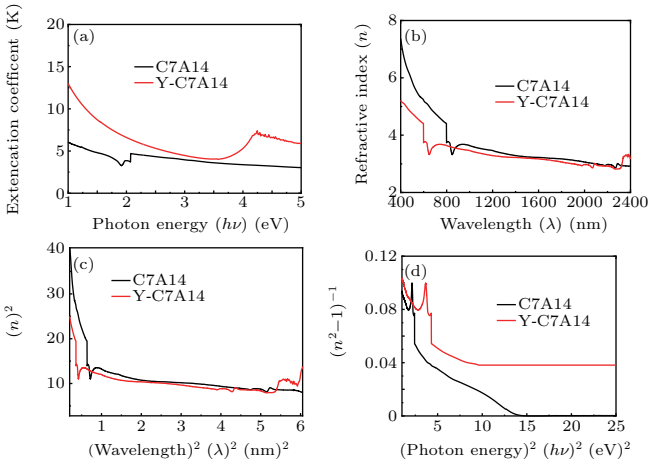


Fig. 3. (a) The relation between k and $h\nu$, (b) the dependence of n on λ, (c) the relation between n^2 and λ and (d) the dependence of $h\nu^2$ and $(n^2-1)^{-1}$ for C12A7and Y-Ca12A7 single crystals.

The extinction coefficient k for all films was calculated from the relation

$$k = \frac{\alpha \cdot \lambda}{4\pi}. \tag{7}$$

The relation between k of these crystals with $h\nu$ is shown in Fig. 3(a). As we can see, doping with Y increases the values of k due to the leakage current that resulted from the rare earth element. The refractive index n for these crystals was calculated as[47]

$$n = \frac{(1+\sqrt{R})}{(1-\sqrt{R})}. \tag{8}$$

Figure 3(b) shows the dependence of n on the wavelength λ for these crystals. From Fig. 3(b), it is clear that, the C12A7 crystals had a higher value of n than Y-Ca12A7crystals. The concept of the single oscillator phenomena of these crystals were studied from the dispersion of n for C12A7 and Y-Ca12A7 single crystals, which can be expressed by the Wemple–DiDomenico relationship[48]

$$n^2(E) - 1 = \frac{E_o E_d}{E_o^2 - E^2}. \tag{9}$$

The values of E_o and E_d for all samples are shown in Table 2. Based on the model parameters E_o and E_d, the M_{-1} and M_{-3} moments were determined by using[49]

$$E_o^2 = M_{-1}/M_{-3}, \tag{10}$$

$$E_d^2 = M_{-1}^3/M_{-3}. \tag{11}$$

Table 2 shows the values of the M_{-1} and M_{-3} for C12A7 and Y-Ca12A7 single crystals. The oscillator strength f was calculated as[50]

$$f = E_o E_d. \tag{12}$$

The value of f increases with doping. The relation between n^2 and λ^2 for the studied thin films is shown in Fig. 3(c). The behavior of the ratio of $(n^2-1)^{-1}$ with $h\nu$ was determined optically as follow:[51]

$$n^2 - k^2 = \varepsilon_L - \left(\frac{e^2 N}{4\pi c^2 \varepsilon_o m^*}\right)\lambda^2. \tag{13}$$

The ratios of free carrier concentration and effective mass N/m^* for these crystals were calculated as shown in Table 2. From this table, it is clear that the doping affects N/m^*. The value of ε_L for these thin films was determined from Fig. 3(d), as the intercept with y-axis[52] as shown in Table 2.

Table 2. The influence of doping on E_d, E_o, ε_L, N/m^*, M_{-1}, M_{-3} and f.

Crystal type	E_o (eV)	E_d (eV)	M_{-1}	M_{-3}	f (eV)^2	N/m^* (gm^{-1}·cm^{-3})	ε_L
$Ca_{12}Al_{14}O_{33}$	8.00	15.00	11.00	4.00	120.00	1.40×10^{49}	12.80
$Y_{0.02}Ca_{11.98}Al_{14}O_{33}$ (Y-C12A7)	8.50	18.00	12.00	3.00	153.00	7.20×10^{48}	11.40

In addition, more important parameters such as dielectric loss ε' and dielectric tangent loss ε'' were determined optically[53]

$$\varepsilon' = (n^2 + k^2), \tag{14}$$

$$\varepsilon'' = \left[(n^2+k^2)^2 - (n^2-k^2)^{0.5}\right]. \tag{15}$$

Figures 4(a) and 4(b) show both of ε' and ε'' for these crystals. From Fig. 4(a), it is clear that the behavior of both of ε' and ε'' with $h\nu$ for these samples is completely inverse, and it was also found that ε' and ε'' for Ca12A7 single crystals are increasing with $h\nu$, while the values of ε' and ε'' for a Y-Ca12A7 single crystals slightly decrease with $h\nu$, as a result of change of electron mobilities.

Both VELF and SELF for these films were determined as[54]

$$\text{VELF} = \frac{\varepsilon''}{\varepsilon'^2 + \varepsilon''^2}, \tag{16}$$

$$\text{SELF} = \frac{\varepsilon''}{(\varepsilon'+1)^2 + \varepsilon''^2}. \tag{17}$$

The relation between VELF/SELF for these crystals is shown in Fig. 4(c). From Fig. 4(c), the values of VELF/SELF for $Ca_{12}Al_{14}O_{33}$ single crystals decrease with $h\nu$, while the values of VELF/SELF for $Y_{0.02}Ca_{11.98}Al_{14}O_{33}$ single crystals increase with $h\nu$.

As a result of its optical application in electronic devices, another important parameter has been determined optically for these crystal, that is the degree of nonlinearity. The third-order nonlinear optical susceptibility $\chi^{(3)}$ depends mainly on $h\nu$ and both of E_o and E_d, and is determined as[55]

$$\chi^{(3)} = A\left[\frac{E_o \cdot E_d}{4\pi(E_o - h\nu)^2}\right]^4, \tag{18}$$

where $A = 1.7\times10^{-10}$ e.s.u.[55] The relation between $\chi^{(3)}$ and $h\nu$ is shown in Fig. 4(d). From Fig. 4(d), it was noticed that both of the crystals had the same behavior with $\chi^{(3)}$, but the values of $\chi^{(3)}$ for Y-Ca12A7 single crystals is higher than Ca12A7 single crystals, as a result of the electron mobitities which allow to increase the ability to absorb incident light beams.

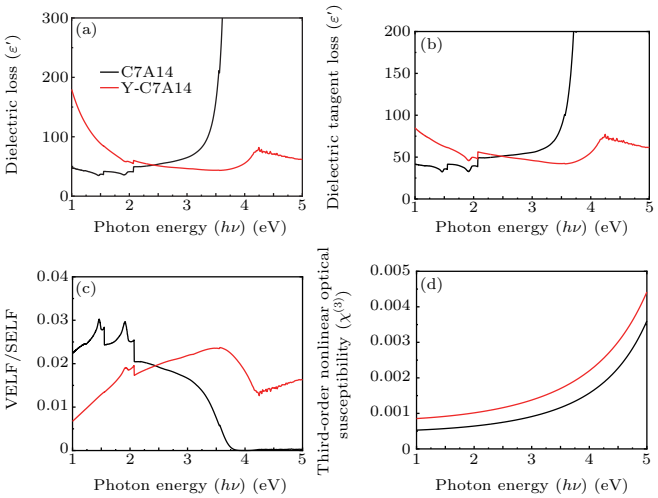


Fig. 4. The influence of $h\nu$ on (a) dielectric loss ε', (b) dielectric tangent loss ε'', (c) the VELF/SELF and (d) $\chi^{(3)}$ for C12A7 and Y-Ca12A7 single crystals.

4. Conclusion

The high quality $Ca_{12}Al_{14}O_{33}$ (C12A7) and $Y_{0.02}Ca_{11.98}Al_{14}O_{33}$ (Y-C12A7) single crystals were prepared by using the TSFZ method. The doping was achieved for this crystal by using Y-element. The doing affected on the structure parameters such as number of defects, lattice strain and number of crystallites, and the doping played an important rule for changing the measured optical parameters such as T and R. The E_{gdir} increases with doping because of the changing of the electron mobility and conductivity. Another optical result such as E_o, E_d and f have been affected by doping. N/m^* decreased on order of magnitude because of the increasing of the electrons number, and on the other hand the doping process had affected strongly on the dielectric results, where the behavior for the dielectric loss and dielectric tangent loss had

completely inverted for these crystals. While the value of $\chi^{(3)}$ had increased by doping. Finally, our results confirmed the doping of Y-ion in C12A7 can be good candidate for optical applications.

References

[1] Exarhos G J and Zhou X D 2007 *Thin Solid Films* **515** 7025
[2] Hosono H 2007 *Thin Solid Films* **515** 6000
[3] Jonas S, Nadachowski F and Szwagierczak D 1999 *Ceram. Int.* **25** 77
[4] Aitasalo T, Holsa J, Jungner H, Lastusaari M, Niittykoski J, Parkkinen M and Valtonen R 2004 *Opt. Mater.* **26** 113
[5] Dongdong J 2006 *J. Lumin.* **117** 170
[6] Murayama Y 1999 *Luminous Paints* (Boca Raton: Phosphor Handbook, CRC Press)
[7] Kang E T, Lee S J and Hannon A C 2006 *J. Non Cryst. Solids* **352** 725
[8] Sampaio J A, Gama S, Baesso M L and Catunda T 2005 *J. Non Cryst. Solids* **351** 1594
[9] Sampaio J A, Catunda T, Coelho A A, Gama S, Bento A C, Miranda L C M and BaessoM L 2000 *J. Non Cryst. Solids* **273** 239
[10] Mazin I I and Papaconstantopoulos D A 2004 *Phys. Rev. B* **69** 180512
[11] Kalita S J, Bose S, Bandyopadhyay A and Hosick H L 2002 *J. Mater. Res.* **17** 3042
[12] Watauchi S, Tanaka I, Hayashi K, Hirano M and Hosono H 2002 *J. Cryst. Grow.* **237–239** 801
[13] Toldsepp E, Avarmaa T, Denks V, Feldbach E, Kirm M, Maaroos A, Mandar H and Vielhauer S 2010 *Optic. Mater.* **32** 784
[14] Gong L, Lin Z, Ning S, Sun J, Shen J, Torimoto Y and Li Q 2010 *Mater. Lett.* **64** 1322
[15] Yuan X, Xu Y and He Y 2007 *J. Alloys Compd.* **441** 251
[16] Jeevaratnam J, Glasser F P and Glasser L S D 1964 *J. Am. Ceram. Soc.* **47** 105
[17] Lacerada M, Irvine J T S, Lachowski E E, Glasserand E P and West A R 1988 *Trans. J.* **87** 191
[18] Hosono H, Hayashi K, Kajihara K, Sushko P V and Shluger A L 2009 *Sol. Stat. Ion.* **180** 550
[19] Matsuishi S, Hayashi K, Hirano M and Hosono H 2005 *J. Am. Chem. Soc.* **127** 12454
[20] Liu X L, Liu Y X, Yan D T, Zhu H C, Liu C G, Xu C S, Liu Y C and Wang X J 2012 *J. Mater. Chem.* **22** 16839
[21] Bartl H and Scheller T 1970 *Mineral. Monatshefte* **35** 547
[22] Christensen A N 1987 *Acta Chem. Scand.* **41a** 110
[23] Strandbakke R, Kongshaug C, Haugsrud R and Norby T 2009 *J. Phys. Chem. C* **113** 8938
[24] Lee D K, Kogel L, Ebbinghaus S G, Valov I, Wiemhoefer H D, Lerch M and Janek J 2009 *Phys. Chem. Chem. Phys.* **11** 3105
[25] Janek J and Lee D K 2010 *J. Korean Ceram. Soc.* **47** 99
[26] Li Q X, Hayashi K, Nishioka M, Kashiwagi H, Hirano M, Torimoto Y, Hosono H and Sadakata M 2002 *Appl. Phys. Lett.* **80** 4259
[27] Labidi M, Labidi S, Ghemid S, Meradji H and El Haj Hassan F 2010 *Phys. Scr.* **82** 045605
[28] Hosono H, Asada N and Abe Y 1990 *J. Appl. Phys.* **67** 2840
[29] Dan W, Yuxue L, Changshan X, Yichun L, Guorui W and Xinghua L 2008 *J. Rar. Eaths.* **26** 433
[30] Park Y J and Kim Y J 2008 *Ceram. Inter.* **34** 1109
[31] Zhu H, Liu Y, Yan D, Bian H, Li S, Liu C, Xu C and Wang X 2014 *Opt. Mater.* **36** 1771
[32] Singh V, Chakradhar R P S, Ledoux-Rak I, Badie L, Pelle F and Ivanova S 2009 *J. Lumin.* **129** 1375
[33] Ju H, Su X, Xu S, Zhang Y, Deng D, Zhao S, Wang H, Wang B and Sun L 2009 *Mater. Lett.* **63** 1275
[34] Lin Y, Tang Z, Zhang Z and Nan C 2003 *J. Europ. Ceram. Soc.* **23** 175
[35] Kumar A S, Kumar R A, Balasundaraprabhu R, Senthil K, Kumar S R and Gunasekaran V 2015 *Spectrochim. Acta A* **134** 283
[36] Rui W, Yushen Z, Jinchao S, Liang L and Yanling X 2011 *J. Rar. Eaths* **29** 826
[37] Verma R K and Rai S B 2013 *Chem. Phys. Lett.* **559** 71
[38] Park J, Kim G and Kim Y J 2013 *Ceram. Inter.* 39 S623
[39] Brika M G, Pan Y X and Liu G K 2011 *J. Alloys Compd.* **509** 1452
[40] Murata T, Tanoue T, Iwasaki M, Morinaga K and Hase T 2005 *J. Lumin.* 114 207
[41] Meng L, Meng H, Gog W, Liu W and Zhang Z 2011 *Thin Solid Films* **519** 7627
[42] Badr Y, Battisha I K, El Nahrawy A M S, Elouadi B and Kamal M 2011 *New Journal of Glass and Ceramics* **1** 71
[43] Gu F., Wang S F, Lu M K, Zhou G J, Xu D and Yuan D R 2004 *J. Phys. Chem. B* **108** 8119
[44] Khan Z R, Zulfequar M and Khan M S 2010 *Mater. Sci. Eng. B* **174** 145
[45] Aranda J, Morenza J L, Esteve J and Codina J M 1984 *Thin Solid Films* **120** 23
[46] Fadel M, Fayek S A, Abou-Helal M O, Ibrahium M M and Shakra A M 2009 *J. Alloys Compd.* **485** 604
[47] Pankove J I 1971 *Optical Process in Semiconductors* (New York: Dover Publications)
[48] Torris J, Cisneros J I, Gordillo G and Alvarez F 1996 *Thin Solid Films* **289** 238
[49] Ali A I, Ammar A H and Abdel Moez A 2014 *Superlatt. Microstruct.* **65** 285
[50] El mandouh Z El Sayed, Elmeleegi H A and Abdel Moez A 2014 *Turk. J. Phys.* **38** 145
[51] Marquez E, Bernal-Oliva A M, Gonzalez-Leal J M, Prieto-Alcon R, Ledesma A, Jimenez-Garay R and Márti I 1999 *Mater. Chem. Phys.* **60** 231
[52] M El-Nahass M, Ammar A H, Farag A A M, Atta A A and El-Zaidia E F M 2011 *Sol. Stat. Sci.* **13** 596
[53] Djurisic A B and Li E H 1998 *Opt. Commun.* **157** 72
[54] Ali A I, Son J Y, Ammar A H, Abdel Moez A and Kim Y S 2013 *Results Phys.* **3** 167
[55] Ziabari A A and Ghodsi F E 2011 *J. Alloys Compd.* **509** 8748